ANTIOXIDANTS & REDOX SIGNALING
Volume 14, Number 11, 2011

DOI: 10.1089/ars.2010.3489

ORIGINAL RESEARCH COMMUNICATION

Disruption of Pyridine Nucleotide Redox Status During Oxidative Challenge at Normal and Low-Glucose States: Implications for Cellular Adenosine Triphosphate, Mitochondrial Respiratory Activity, and Reducing Capacity in Colon Epithelial Cells

Magdalena L. Circu, Ronald E. Maloney, and Tak Yee Aw

Abstract

We recently demonstrated that menadione (MQ), a redox cycling quinone, mediated the loss of mitochondrial glutathione/glutathione disulfide redox balance. In this study, we showed that MQ significantly disrupted cellular pyridine nucleotide (NAD^+/NADH, $NADP^+$/NADPH) redox balance that compromised cellular ATP, mitochondrial respiratory activity, and NADPH-dependent reducing capacity in colonic epithelial cells, a scenario that was exaggerated by low glucose. In the cytosol, MQ induced NAD^+ loss concurrent with increased $NADP^+$ and NAD kinase activity, but decreased NADPH. In the mitochondria, NADH loss occurred in conjunction with increased nicotinamide nucleotide transhydrogenase activity and $NADP^+$, and decreased NADPH. These results are consistent with cytosolic NAD^+-to-$NADP^+$ and mitochondrial NADH-to-NADPH shifts, but compromised NADPH availability. Thus, despite the sacrifice of NAD^+/NADH in favor of NADPH generation, steady-state NADPH levels were not maintained during MQ challenge. Impairments of cellular bioenergetics were evidenced by ATP losses and increased mitochondrial O_2 dependence of pyridine nucleotide oxidation–reduction; half-maximal oxidation (P_{50}) was 10-fold higher in low glucose, which was lowered by glutamate or succinate supplementation. This exaggerated O_2 dependence is consistent with increased O_2 diversion to non-mitochondrial O_2 consumption by MQ-semiquinone redox cycling secondary to decreased NADPH-dependent MQ detoxication at low glucose, a situation that was corrected by glucose-sparing mitochondrial substrates. *Antioxid. Redox Signal.* 14, 2151–2162.

Introduction

Pyridine nucleotides collectively comprise of reduced and oxidized nicotinamide adenine dinucleotide ($NADH/NAD^+$) and reduced and oxidized nicotinamide adenine dinucleotide phosphate ($NADPH/NADP^+$). While $NADH/NAD^+$ and $NADPH/NADP^+$ possess similar redox potential (~ -400 mV) capable of participating in similar redox-dependent cellular processes, each redox couple is designed to serve different cellular functions. The $NADH/NAD^+$ couple is central in ATP production through electron transfer to the mitochondrial respiratory chain, whereas the $NADPH/NADP^+$ couple functions primarily in biosynthetic and detoxication reactions. In addition, through the transfer of reducing equivalents, NADPH regulates the homeostasis of cellular glutathione/glutathione disulfide (GSH/GSSG) and thioredoxin/thioredoxin disulfide redox systems (6, 7). Based on the estimated rate of maximal electron flow through the $NADH/NAD^+$ and $NADPH/NADP^+$ couples (36), the NADH-utilizing mitochondrial respiratory chain and NADPH-linked redox processes are viewed as representing high-flux and low-flux electron transfer pathways, respectively (16). As such, perturbations in the cellular NADH and NADPH status are expected to majorly disrupt ATP generation and NADPH-dependent detoxication reactions and other metabolic pathways that are mediated by high-flux (NADH) and low-flux (NADPH) electron transfers (16).

Recent studies from our laboratory have demonstrated that treatment of HT29 and NCM460 colonic epithelial cells with menadione (MQ), a redox cycling quinone, induced a significant loss of cellular and mitochondrial GSH/GSSG redox balance (9) that was associated with oxidative damage to

Department of Molecular and Cellular Physiology, Louisiana State University, Health Sciences Center, Shreveport, Louisiana.

mitochondrial DNA (8), and activation of mitochondrial apoptotic signaling. Given that the control of GSH/GSSG redox homeostasis is intricately tied to NADPH/$NADP^+$ redox status, we sought, in this study, to investigate the effect of MQ on cytosolic and mitochondrial NADPH/$NADP^+$ and NADH/NAD^+ and to define the metabolic impact of a disrupted pyridine nucleotide status in terms of cellular ATP status and reducing capacity, and mitochondrial respiratory (oxidation–reduction) activity. Given that glucose is a central metabolic substrate in NADH and NADPH maintenance, we further examined the influence of low glucose on MQ-induced pyridine nucleotide changes. Activities of various NADH- and NADPH-generating enzymes, such as $NADP^+$/NAD^+-dependent isocitrate dehydrogenase (ICDH) (14, 19), glucose-6-phosphate dehydrogenase (G6PDH) (13), malic enzyme (ME) (27), NAD kinase (NADK) (25), and mitochondria-associated transhydrogenase (nicotinamide nucleotide transhydrogenase [NNT]) (11), previously shown to maintain NADH/NADPH levels, were also determined.

Our working hypothesis, as summarized in Figure 1, proposed that the high rate of NADPH consumption in MQ metabolism in HT29 cells through either a one-electron reduction in MQ-semiquinone ($SQ^\bullet$) redox cycling or a two-electron reduction in MQ-to-hydroquinone (HQ) formation would impose a considerable demand on cellular NADPH supply. This NADPH drain would cause a series of acute metabolic compensations in favor of NADPH generation, including NAD^+/NADH-to-$NADP^+$/NADPH conversion and stimulation of NADPH-generating enzyme activities. The consequent shifts in pyridine nucleotide status are expected to perturb mitochondrial bioenergetics and cellular supply of reducing equivalents. The results of the current study support our hypothesis that MQ-mediated cytosolic and mitochondrial pyridine nucleotide changes that favor NADPH production. Decreases in cellular ATP occurred concurrently with the sacrifice of mitochondrial NADH, and excessive MQ-induced NADPH and O_2 utilization resulted in overall decreases in cellular reducing capacity and associated GSH/GSSG imbalance, and compromised mitochondrial oxidation–reduction activity, respectively. The dramatic exaggeration in NADH and NADPH loss and mitochondrial impairment under glucose-limiting conditions underscore the importance of this central substrate in intermediary metabolism and pyridine nucleotide redox homeostasis in colonic epithelial cells.

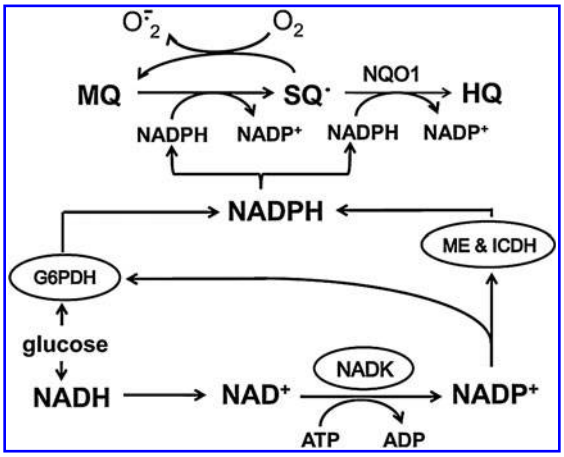

FIG. 1. MQ metabolism through a one-electron reduction in MQ-$SQ^\bullet$ redox cycling or NQO1-catalyzed two-electron reduction in MQ-to-HQ formation imposes a high demand on cellular NADPH supply. NADPH drain results in metabolic responses that support NADPH generation, such as the sacrifice of the NAD^+/NADH redox pools in favor of $NADP^+$ and NADPH generation and the stimulation of activities of NADPH-generating enzymes. MQ, menadione; $SQ^\bullet$, semiquinone radical; HQ, hydroquinone; NQO1, NAD(P)H quinone oxidoreductase, also known as DT diaphorase; $O_2^{\bullet-}$, superoxide; G6PDH, glucose 6-phosphate dehydrogenase; ME, malic enzyme; ICDH, isocitrate dehydrogenase; NADK, NAD kinase.

Materials and Methods

Materials

The following chemicals were from Sigma Chemical Company: Brij 35, lysolecithin, 3-acetylpyridine adenine nucleotide, glutathione, glutathione disulfide, iodoacetic acid, isocitrate, NAD^+, NADH, $NADP^+$, NADPH, acetyl coenzyme A, α-ketoglutaric acid, malate, glucose-6-phosphate, MQ, alcohol dehydrogenase, G6PDH, phenazine ethosulfate, Tris-HCl, 3-(4,5-dimethylthiazol-2yl)-2,5-diphenyltetrazolium bromide, nicotinamide, glutamate, dicumarol, and succinate. Antibiotic/antimycotic, trypsin, L-glutamine, McCoys' medium, and Dulbecco's modified essential medium (DMEM) were from Gibco Corporation, and fetal bovine serum (FBS) was from Atlanta Biologicals. The protein dye assay kit was from Biorad Corporation. All other chemicals were of reagent grade and were purchased from local sources.

Methods

HT29 cell culture and cell incubations. HT29 cell line, a human colon epithelial cell line derived from the adenocarcinoma of the colon of a female Caucasian (40), was purchased from American Type Culture Collection. Cells were grown in McCoy's medium supplemented with penicillin (100 units/ml), streptomycin (100 units/ml), and 10% FBS. The McCoy's medium contains 3 g/l (18.3 m*M*) glucose, the standard and normal glucose concentration for optimal HT29 cell growth in culture. HT29 cells were maintained at 37°C in 5% CO_2 humidified incubator. Unless otherwise stated, confluent cells in T75 flasks were harvested and were seeded at the specified densities the day before, and on the day of the experiment, media were replaced by serum-free DMEM to avoid serum antioxidant effects. Cells were incubated for different periods of time with MQ at final concentrations of 50 or 200 μM without significant cell death. Glucose effects were examined using medium concentrations of 3, 0.75, or 0.2 g/l, which corresponded to 18.3, 4.6, or 1.2 m*M*, respectively. Glucose uptake measurements demonstrated that cell-associated glucose levels were equivalent to these medium glucose concentrations (data not shown).

Extraction and assay of total oxidized and reduced pyridine nucleotides. Cellular NAD^+, $NADP^+$, NADH, and NADPH were determined in cell lysates prepared by a single extraction procedure (37). HT29 cells (5×10^6) in DMEM containing 1.2 or 18.3 m*M* glucose were exposed to 50 or 200 μM MQ for 30 or 60 min. Thereafter, cells were washed in phosphate-buffered saline and scrapped into extraction buffer containing

20 m*M* $NaHCO_3$, 100 m*M* Na_2CO_3, and 10 m*M* nicotinamide. The cells were quickly frozen in liquid nitrogen and thawed in at 37°C. Cell extracts were centrifuged (12,000 *g*, 4°C) and divided into two aliquots. Total contents of NADH plus NAD^+ and NADPH plus $NADP^+$ were determined in the first aliquots by specific enzyme cycling assays (24, 41). The second aliquot was heated at 60°C, 30 min in the dark to selectively decompose NAD^+ and $NADP^+$ followed by NADH and NADPH determination (24, 41). Concentrations of NAD^+ and $NADP^+$ were represented by the difference between the values of the heated and unheated samples. The final concentrations were calculated based on reaction velocities of known standards. All measurements were performed in the dark within 1 h after preparation of cell extracts.

Determination of cytosolic and mitochondrial pyridine nucleotides

Cell incubations and digitonin fractionation. HT29 cells (1×10^7cells/ml) were suspended in round-bottom flasks in Krebs-Henseleit-bicarbonate buffer, pH 7.4, containing 1.2 or 18.3 m*M* glucose (9). After 30 min equilibration at 37°C, cells were treated with 50 or 200 μM MQ. At designated times, 500 μl aliquots (5×10^6 cells) were sampled for digitonin fractionation (2) in the presence of 0.2 *M* KCN to stabilize the pyridine nucleotides as nicotinamide-cyanide derivatives (17). Separation of cytosolic and mitochondrial fractions was performed in 1.5 ml microfuge tubes containing, from the bottom, 100 μl 10% glycerol-KCN, 500 μl silicone oil–mineral oil mixture (4/1, v/v), and 100 μl 1.2 mg/ml digitonin solution (2). Cell aliquots were rapidly mixed with the digitonin layer and centrifuged for 3 min at 14,000 *g*. The supernatants (cytosolic fractions) were mixed 1-to-1, and the bottom mitochondrial layers were diluted 1-to-3 with 0.2 *M* KCN. Nicotinamide-cyanide derivatives were quantified by high-performance liquid chromatography (HPLC) (17).

HPLC analyses. Samples were further derivatized on ice (5 min) with 0.2 *M* KCN buffer containing 0.06 *M* KOH and 1 m*M* bathophenanthroline-disulfonic acid. Mitochondrial samples were extracted with chloroform, and DNA was removed in the lipid-free extracts by centrifugal filtration at 14,000 *g* (Amicon Ultra filters; Millipore Corporation). The filtrates were mixed with 0.2 *M* ammonium acetate/4%(v:v) MeOH, pH 6.0, and the derivatives were separated on a reversed-phase C18 column (250×4.6 mm) and detected at 328 nm (Gilson 118 UV/Vis detector). Pyridine nucleotide levels were quantified by comparison to standards. Mitochondrial samples were analyzed immediately after derivatization due to nucleotide decay upon storage, whereas more stable cytosolic nucleotides were frozen in liquid nitrogen for next-day analyses. HPLC determination of GSH and GSSG levels in cytosolic and mitochondrial fractions were as previously described (9, 29).

ATP determination. Cellular ATP contents were determined using a luciferin/luciferase bioluminescence Promega kit according to the manufacturer's protocol. HT29 cells (1×10^4) were seeded in 96-well plates. The next day, the media were replaced by FBS-free DMEM containing different glucose concentrations, and the cells were exposed to 50 or 200 μM MQ for 30 min; in time course experiments MQ treatment was for 0–60 min. Mitochondria- and glycolysis-derived ATP were determined in the presence of antimycin A (2 μM) and 2-deoxyglucose (2DG), respectively. Molar ratios of 2.5-to-1 of 2DG-to-glucose were used. At designated times, incubation media were removed and equal volumes of lysis buffer containing the luciferase reagent were added to cell monolayers. After 20 min of incubation, luminescence signals proportional to ATP concentrations were quantified using a BMG-Fluostar Optima plate reader. Six-to-eight replicates were conducted for four to six separate cell preparations. ATP contents are expressed as percent relative to controls (100%).

Preparation of cell extracts and assay of enzyme activities and lactate levels. After 30 min of MQ treatment, cells (5×10^6) were harvested and resuspended in homogenization buffer (20 m*M* Hepes, pH 7.4; 0.25 *M* sucrose; and 1 m*M* ethylenediaminetetraacetic acid and protease inhibitors) and frozen in liquid nitrogen. Samples were thawed, sonicated, and subjected to a 250 *g* (10 min) followed by a 20,000 *g* (30 min) centrifugation step at 4°C to obtain cytosolic fractions. Mitochondrial pellets collected at this centrifugation step were taken into 100 μl homogenization buffer. Extracts were used on the same day or stored at −80°C for enzyme assays. Activities of cytosolic enzymes—$NADP^+$-linked ME, $NADP^+$-linked ICDH, and G6PDH as well as mitochondrial NAD^+- and $NADP^+$-dependent ICDH—were determined spectrophotometrically by enzyme-coupled assays (3, 10, 27). NADK activity was determined in a two-step procedure (26), and kinase activity is expressed as enzyme units; one unit is the amount of enzyme generating 1 μmol of $NADP^+$ per minute at 30°C. Intact mitochondria prepared from $\sim30\times10^6$ cells (15) were used for NNT assay. The transhydrogenase activity, assayed as reduction of oxidized 3-acetylpyridine adenine nucleotide by NADPH at 375–400 nm, was performed using dual-wavelength spectrophotometry (30). Cytosolic lactate levels were determined by an enzyme-coupled assay using dual-wavelength spectrophotometry (21).

Oxygen dependence of oxidation–reduction of pyridine nucleotides. HT29 cells (5×10^6/ml) were suspended in modified Gey's buffer containing 0, 1.2, 4.6, or 18.3 m*M* glucose and treated with 50 μM MQ. Whenever present, glutamate and succinate were at 10 m*M* and Dicumarol at 0.1 μM final concentrations. Oxidation–reduction of mitochondrial pyridine nucleotides was performed by dual-wavelength spectrophotometry in an AMINCO DW-2000 spectrophotometer (4). Briefly, cells in 5-ml buffer were kept in suspension by gentle stirring. Solution O_2 was measured using a Clark-type O_2 electrode calibrated with respect to air (21% O_2) or 100% O_2 that was inserted through the cover of the incubation vessel. The gaseous phase of the vessel was purged with prepurified argon to allow the cells to become anaerobic transiently, after which known volumes of 21% O_2 or 100%-saturated buffer were added using a Hamilton syringe to obtain the desired O_2 concentrations in solutions. Changes in oxidation–reduction of pyridine nucleotides from anaerobic-to-aerobic transitions were measured at the wavelength pair 340–375 nm, and expressed as P_{50} values, defined as the O_2 concentrations at half maximal oxidation.

Protein assay. Protein was measured using Bio-Rad Assay kit according to manufacturer's protocol.

Statistical analysis. Results are expressed as mean ± standard error of the mean. Data were analyzed by one-way analysis of variance statistical analysis with Bonferroni's post-test for multiple comparisons. $p < 0.05$ was considered statistically significant.

Results

MQ disrupts pyridine nucleotide status that is exacerbated by low glucose

The time course of MQ effect on cellular pyridine nucleotides in the presence of 18.3 m*M* glucose is illustrated in Figure 2A. MQ at 50 and 200 μM equally decreased cellular NADH at 30 and 60 min, whereas significant decreases in NADPH occurred only at 200 μM MQ at 60 min. NAD^+ contents were unaffected at 50 μM MQ at all times, but were significantly lower at 200 μM at 60 min. Cellular $NADP^+$ levels were essentially unchanged, although there was a trend toward an increase at 200 μM at 60 min. Figure 2B shows that at 30 min, MQ decreased cytosolic NAD^+; at 200 μM MQ NAD^+ levels were down by 85% (solid bars, panel a). Interestingly, MQ was without effect on mitochondrial NAD^+ regardless of dose (panel c). In contrast, mitochondrial NADH levels were dose-dependently sensitive to MQ treatment (panel c), whereas cytosolic NADH, which was ~3% of mitochondrial values, remained low without or with MQ exposure (panel a). In comparison, MQ elicited similar dose-dependent decreases in cytosolic and mitochondrial NADPH and increases in $NADP^+$ levels (panels b and d). However, the quantitative shifts in NADPH and $NADP^+$ were consistently greater in the cytosol.

Since glucose is a major contributor to the maintenance of NADH and NADPH homeostasis, we examined the impact of low glucose (1.2 m*M*). Figure 3A shows that under low-glucose conditions, 50 μM MQ elicited significant decreases in cellular NADH that were similar to those at 18.3 m*M* glucose; however, NADH decreases were exaggerated at 200 μM MQ (15% of basal levels at 30 and 60 min). While NAD^+ levels were minimally altered by 50 μM MQ, significant loss of NAD^+ occurred with 200 μM at both times. The most dramatic changes were seen in NADPH levels that were essentially depleted by 60 min, regardless of MQ dose. Concurrent with MQ-induced NADPH decreases were time-dependent increases in $NADP^+$ levels. Figure 3B shows that MQ-induced decreased NAD^+ and NADPH, and increased $NADP^+$ in the cytosol was highly exaggerated. Notably, NAD^+ and NADPH decreases at 1.2 m*M* glucose were achieved at 50 μM MQ (panels a and b). In the mitochondria, MQ elicited significant decreases in NADH and NADPH levels that were paralleled by increases in $NADP^+$ (Fig. 3B, panels c and d), responses that were exacerbated as compared to 18.3 m*M* glucose. In contrast to a relatively stable mitochondrial NAD^+ pool in the presence of glucose abundance (Fig. 2B), MQ induced a fall in mitochondrial NAD^+ at low glucose, achieving statistical significance at 200 μM MQ (Fig. 3B, panel c). It is notable that, in the absence of MQ stress, cells in 1.2 m*M* glucose (Fig. 3B) exhibited lower baseline levels of cytosolic NADPH and mitochondrial NADH, but higher contents of mitochondrial NADPH than cells in normal glucose (Fig. 2B); this indicates that decreased glucose availability *per se* is a limiting factor in the metabolic production of cytosolic NADPH and mitochondrial NADH.

MQ stimulates activities of cytosolic and mitochondrial NADPH-generating enzymes

The cellular sources of NADPH include $NADP^+$-linked dehydrogenases, mitochondria-associated pyridine nucleotide transhydrogenase, and the pentose phosphate pathway (PPP), a quantitatively significant supplier of cytosolic NADPH (3, 18, 32). Given that MQ metabolism is associated with increased demand for NADPH (Fig. 1), activities of various NADPH-generating systems were determined (Table 1). The results show that the most notable change was the increase in NADK activity that occurred at both MQ doses and at all glucose levels; this increase in kinase activity is consistent with elevating

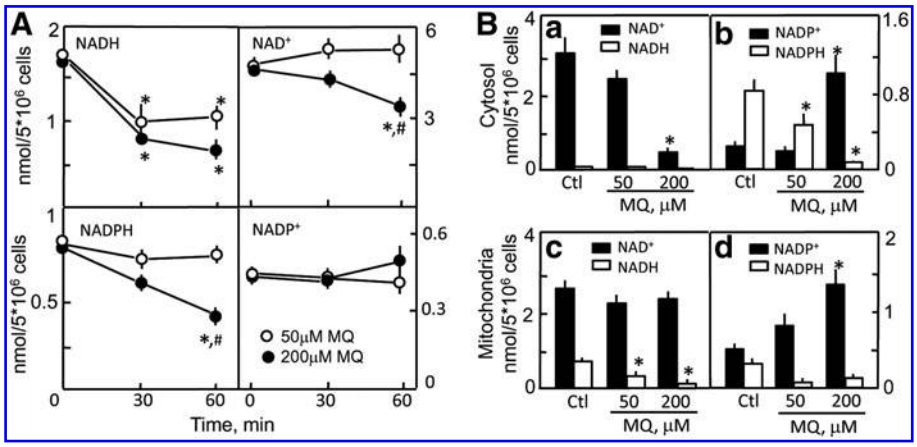

FIG. 2. MQ-induced changes in NADH/NAD^+ and NADPH/$NADP^+$ contents in HT29 cells under normal glucose conditions. (A) Time course of pyridine nucleotide changes. Cells (5×10^6) were treated with 50 or 200 μM MQ for 30 and 60 min in 3 g/l glucose. At designated times, cell aliquots were removed, total cell lysates were prepared, and cellular contents of NADH plus NAD^+ and NADPH plus $NADP^+$ were determined by enzyme cycling assays. Nucleotide contents were calculated based on reaction velocities of known standards. Results are mean ± SEM for 5 cell preparations. $^*p < 0.05$ versus untreated controls (zero time); $^\#p < 0.05$ versus 50 μM MQ. **(B)** Changes in cytosolic **(a, b)** and mitochondrial **(c, d)** NADH/NAD^+ and NADPH/$NADP^+$. Cells (5×10^6) were incubated with 50 or 200 μM MQ in 3 g/l (18.3 m*M*) glucose for 30 min. At the end of the incubation, cytosolic and mitochondrial fractions were prepared by digitonin fractionation as described in the Methods section. KCN (0.2 *M*) was added to stabilize the pyridine nucleotides as nicotinamide-cyanide derivatives, which were separated by high-performance liquid chromatography. Nucleotide contents were quantified by comparison to authentic standards derivatized in the same manner. Results are expressed as nmol per 5×10^6 cells and are mean ± SEM for four cell preparations. $^*p < 0.05$ versus untreated controls. SEM, standard error of the mean.

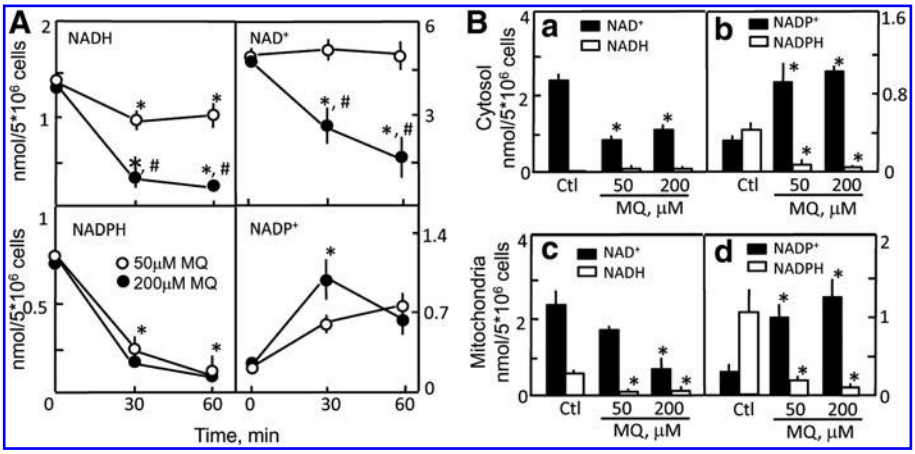

FIG. 3. MQ-induced changes in NADH/NAD$^+$ and NADPH/NADP$^+$ contents in HT29 cells under low-glucose conditions. Cells (5×10^6) were treated with 50 or 200 μM MQ in 0.2 g/l (1.2 mM) glucose. Time course of changes in total pyridine nucleotides **(A)**, and determination of cytosolic and mitochondrial contents **(B)** were performed as described in Figure 2. Results are expressed as nmol per 5×10^6 cells and are mean ± SEM for three cell preparations for total content and four cell preparations for cytosolic and mitochondrial contents. $^*p < 0.05$ versus untreated controls; $^\#p < 0.05$ versus 50 μM MQ.

NAD$^+$-to-NADP$^+$ phosphorylation. Interestingly, basal NADK activity itself was attenuated with decreasing glucose. The activity of G6PDH was significantly elevated at 200 μM MQ, whereas cytosolic NADP$^+$-linked ICDH and ME were minimally altered from untreated controls. Neither mitochondrial NAD$^+$ or NADP$^+$-dependent ICDH activities were much affected by MQ or glucose status although there was a trend toward higher activities of NAD$^+$-ICDH with decreasing glucose. In comparison, NNT activity increased at both MQ doses, achieving significance at 200 μM MQ at low glucose. These results suggest that NNT-mediated NADH-to-NADPH transhydrogenation and the pentose phosphate shunt were important pathways in NADPH generation during MQ challenge.

MQ and low glucose disrupts GSH/GSSG redox status

Since NADPH availability is central to GSH/GSSG homeostasis, the impact of MQ on GSH/GSSG status was studied under normal and low-glucose conditions. Figure 4A shows that at 18.3 mM glucose, cytosolic GSH and GSSG levels were minimally affected at both MQ doses. Similarly, mitochondrial GSH/GSSG status was unaltered at 50 μM MQ, but 200 μM MQ induced time-dependent decreases in mitochondrial GSH, achieving significance as early as 15 min. These GSH decreases were paralleled by GSSG increases. Thus, even with glucose abundance, the mitochondrial GSH pool was vulnerable to high MQ dose, in agreement with our recent findings (8, 9). In contrast, cytosolic and mitochondrial GSH pools were equally sensitive to both MQ doses under glucose-limiting conditions (Fig. 4B). Notably, 200 μM MQ elicited maximal GSH loss and GSSG increase within 15 min, and GSH/GSSG disruption by 50 μM MQ was evident at 30 and 60 min. Significantly, the time- and dose-dependent changes in GSH and GSSG and their sensitivity to low glycemic status mirrored the changes in NADPH under similar conditions (Figs. 2 and 3).

MQ and low glucose decreases cellular ATP levels and increases O_2 dependence of oxidation–reduction of pyridine nucleotides

The impact of MQ on cellular bioenergetics was assessed by changes in ATP contents and mitochondrial respiratory (oxidation–reduction) activity.

Cellular ATP levels. Figure 5A shows that at 18.3 mM glucose, MQ at 50 or 200 μM induced time-dependent decreases in cellular ATP that mirrored the losses of NADH (Fig. 2A). Treatment of control cells with either antimycin A or 2DG revealed that glycolysis-derived ATP accounted for ~50% of total cellular ATP contents (Fig. 5B), indicating that these cancer cells rely heavily on aerobic glycolysis for ATP generation within the cytosol, consistent with the Warburg effect (39). Figure 5B (top panel) illustrates the changes in mitochondria-derived ATP (antimycin A sensitive). The results show that glucose-limiting conditions alone (4.6 and 1.2 mM) induced 15%–20% decreases in baseline mitochondrial ATP levels, which were further decreased by MQ treatment. Interestingly, mitochondrial ATP contents at 18.3 and 4.6 mM glucose after 50 μM MQ treatment fell to levels of those at 1.2 mM, which was unchanged from its baseline value. In comparison, 200 μM MQ treatment induced > 60% loss of basal ATP at 1.2 mM glucose, whereas ATP values at 18.3 and 4.6 mM glucose remained at 60%–70% of basal values regardless of MQ dose. These results indicate that mitochondrial ATP is sensitive to cellular glucose status and that MQ exacerbates ATP loss at low glucose.

Figure 5B (bottom panel) illustrates the changes in glycolysis-derived ATP (2DG sensitive) representing cytosolic ATP. The results show that cytosolic ATP was increased ~10% by low-glucose conditions alone, a magnitude of change that mirrored the loss in mitochondrial ATP (panel a). Cytosolic ATP consistently fell by ~30% under normal and intermediate glucose conditions regardless of MQ dose. A similar 30% loss in cytosolic ATP was elicited by 50 μM MQ at 1.2 mM glucose; however, ATP fell by 80% at 200 μM MQ, suggesting that glycolytic activity was either inhibited, or limited by glucose availability. To test this, we measured cytosolic lactate formation. The results in Figure 5C show the presence of high basal lactate levels, consistent with aerobic glycolysis, the Warburg effect. Significantly, lactate formation at 4.6 and 18.3 mM glucose was dose-dependently increased by MQ, indicating that aerobic glycolysis was greatly stimulated (2- to 2.5-fold) by MQ stress under conditions of glucose abundance. In contrast, increases in lactate production were substantially reduced under glucose-limiting conditions at 1.2 mM glucose and high MQ stress (200 μM) (Fig. 5C).

Table 1. Menadione Effect on Activities of Key Mitochondrial and Cytosolic-Oxidized Nicotinamide Adenine Dinucleotide-Linked and Oxidized Nicotinamide Adenine Dinucleotide Phosphate-Linked Dehydrogenases Under Various Glucose Concentrations

	18.3 mM glucose + MQ (μM)			*6.1 mM glucose + MQ (μM)*			*1.2 mM glucose + MQ (μM)*		
Cellular enzymes	*0*	*50*	*200*	*0*	*50*	*200*	*0*	*50*	*200*
cyto NADK (U/min/mg prot)	1.1 ± 0.07	1.36[a] ± 0.08	1.29[a] ± 0.05	0.98 ± 0.05	1.67[b] ± 0.1	1.76[b] ± 0.08	0.46[c] ± 0.05	0.56 ± 0.06	0.82[b] ± 0.05
cyto ICDH-$NADP^+$ (nmol/min/mg prot)	78.55 ± 3.8	76.9 ± 2.9	71.1 ± 3	82.88 ± 6.8	82.75 ± 3.9	75.57 ± 5	54.53[c] ± 3	58.9[c] ± 2.8	65.1 ± 4.3
cyto ME-$NADP^+$ (nmol/min/mg prot)	26.87 ± 2.9	30.2 ± 2.9	26.8 ± 3	28.88 ± 2.3	36.8[a] ± 1.7	36.27[a] ± 3.1	23.9 ± 2.2	27.9 ± 4	36.5 ± 8.8
cyto G6PDH (nmol/min/mg prot)	58.2 ± 5.5	74.7 ± 20.9	66.6 ± 22.1	55.79 ± 4.6	62.2 ± 3.7	53.01 ± 3	39.16 ± 2	44.6 ± 3.7	55.5[a] ± 7.7
mito ICDH-NAD^+ (nmol/min/mg prot)	326.3 ± 24.6	308.8 ± 13.9	305.9 ± 14.8	297.1 ± 25.9	358.3[a] ± 14.2	341.9[a] ± 19	359 ± 43	423 ± 123	441 ± 135
mito NNT (nmol/min/mg prot)	5.8 ± 0.4	8.8 ± 2.0	14.1 ± 4.4	nd	nd	nd	6.7 ± 0.7	11.5 ± 2.5	21.8[a] ± 3.6
mito ICDH-$NADP^+$ (nmol/min/mg prot)	280.9 ± 22.2	271.61 ± 14.9	251.7 ± 13.6	263.03 ± 12	310.9 ± 20	268.3 ± 18.8	285.5 ± 15	316.7 ± 18	267.1 ± 58

Cell incubations with MQ under different glucose conditions, preparation of cell lysates, and enzyme assays were as described in Methods. With the exception of NADK and NNT, all enzyme activities are expressed as the amount of NADPH or NADH produced per minute per milligram protein. NADK activity is expressed in Units; one Unit is the amount of enzyme generating 1 μmol of $NADP^+$ in 1 min at 30°C. NNT activity is expressed as nmol of 3-acetylpyridine adenine nucleotide reduced per minute per milligram protein. Results are mean ± standard error of the mean for six separate cell preparations for all enzymes and three preparations for NNT.

[a] $p < 0.05$.

[b] $p < 0.001$ are statistically different from untreated controls at each glucose concentration.

[c] $p < 0.05$ at 0.2 g/l glucose are statistically different from 3 g/l glucose.

MQ, menadione; NADK, NAD kinase; ICDH, isocitrate dehydrogenase; ME, malic enzyme; G6PDH, glucose 6-phosphate dehydrogenase; NNT, nicotinamide nucleotide transhydrogenase; cyto, cytosolic; mito, mitochondrial; nd, not determined.

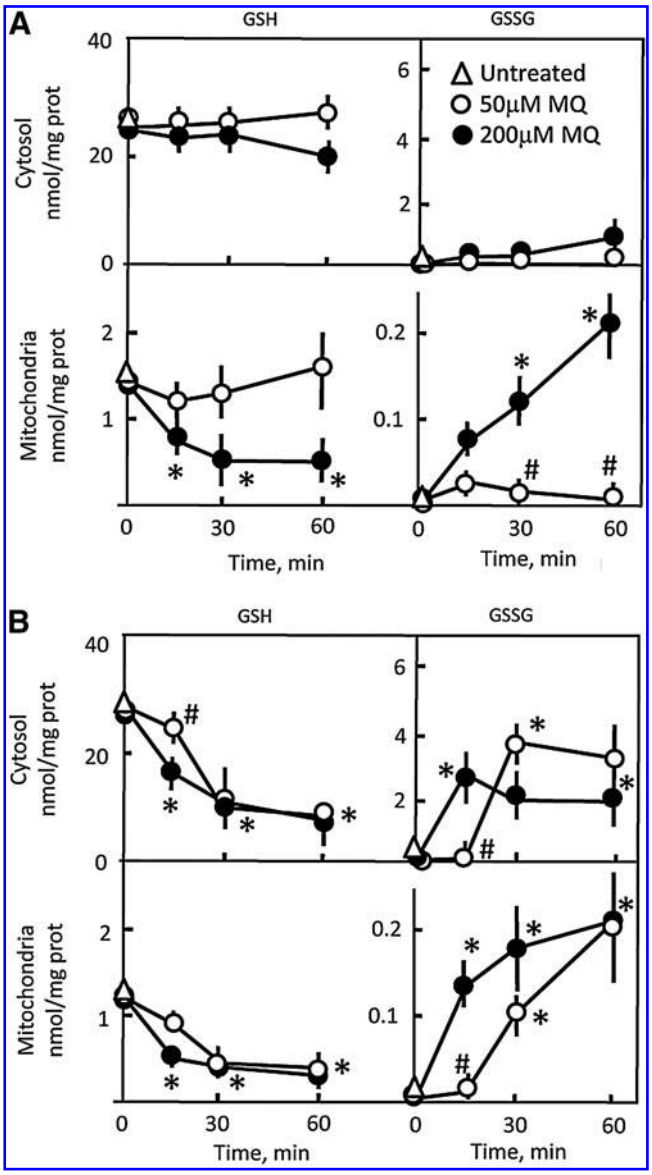

FIG. 4. Time course of changes in cytosolic and mitochondrial GSH and GSSG levels in HT29 cells exposed to MQ under normal glucose conditions (A) and low-glucose conditions (B). Cells (1×10^7/ml) were incubated with 50 or 200 μM MQ in buffer containing either 18.3 mM or 1.2 mM glucose for different times. Cytosolic and mitochondrial fractions were prepared by digitonin fractionation as described in Methods. GSH and GSSG levels were measured by high-performance liquid chromatography as previously described (9) and expressed as nmol/mg protein. Results are mean ± SEM for three cell preparations. $^*p < 0.05$ versus untreated controls; $^\#p < 0.05$ versus 200 μM MQ. GSH, glutathione; GSSG, glutathione disulfide.

Oxidation–reduction of cellular pyridine nucleotides. The integrity of the mitochondrial respiratory activity was evaluated by examining the O_2 dependence of oxidation–reduction of pyridine nucleotides (NAD^+/NADH). Mitochondrial NADH levels were at least 30-fold higher than cytosolic NADH (Figs. 2B and 3B), and cytosolic NADH was depleted due to MQ-induced increase in cytosolic lactate (Fig. 5C); thus, the O_2 dependence reflected oxidation of mitochondrial reducing equivalents. Figure 6A illustrates the O_2 dependence under different glucose conditions. At normal glucose, the P_{50} was 0.4 μM O_2. Treatment with 50 μM MQ induced a right shift in the O_2 dependence and ~2-fold increase in P_{50} (0.7 μM O_2). Significantly, the O_2 dependence at 1.2 mM glucose was shifted to the far right with a P_{50} value of 11.5 μM O_2. Interestingly, cells at intermediate glucose (4.6 mM) elicited an unique O_2 dependence response that resembled cells in 18.3 mM glucose between O_2 concentrations of 0.1 and 1 μM, and cells in 1.2 mM glucose between O_2 concentrations of 10 and 40 μM O_2 with an inflection phase between 1 and 10 μM O_2. These results are consistent with the notion that the increase in P_{50} value was consequent to enhanced O_2 utilization by MQ-$SQ^\bullet$ redox cycling, a scenario that was exaggerated under glucose-limiting conditions. The results in Figure 6B confirmed that MQ-induced O_2 consumption at saturating [O_2] and [O_2] at P_{50} values were, indeed, significantly higher at 1.2 and 4.6 mM glucose than at normal glucose (18.3 mM).

Since MQ metabolism and O_2 dependence of pyridine nucleotides were sensitive to glucose status, we examined whether the addition of succinate or glutamate as alternate fuel for mitochondrial respiration could spare glucose and thereby alter the O_2 dependence profile at decreased (4.6 mM) glucose. Figure 6C shows that exogenous glutamate or succinate addition shifted the O_2 dependence responses to the left of that of glucose alone; the resultant respective P_{50} values of 1.2 μM O_2 and 1.9 μM O_2 were down from 4.8 μM O_2. These results support our reasoning that by providing alternate substrates for the mitochondria, glucose may be spared for the generation of NADPH in MQ detoxication, thereby decreasing MQ-$SQ^\bullet$ cycling and preventing excessive O_2 consumption not associated with mitochondrial respiration. To confirm that HQ formation was the major cytosolic MQ detoxication pathway, cells in normal glucose were pretreated with dicumarol, an inhibitor of DT diaphorase that catalyzes 2-electron reduction of MQ to HQ (Fig. 1). The results show that dicumarol significantly shifted the O_2 dependence to the far right (P_{50} of 8.9 μM O_2, Fig. 6D), a response that was similar in magnitude to cells in 1.2 mM glucose (Fig. 6A). Thus, attenuating MQ detoxication either through DT diaphorase inhibition or through limiting glucose for NADPH generation would increase MQ availability and favor MQ-$SQ^\bullet$ cycling.

Discussion

The current study demonstrated that MQ, a redox cycling quinone, significantly disrupted cellular pyridine nucleotide redox status in HT29 colonic epithelial cells. Loss of pyridine nucleotide homeostasis occurred in conjunction with compromised cellular bioenergetics and mitochondrial respiratory activity as well as with decreased NADPH-dependent reducing capacity and GSH/GSSG redox imbalance. Taken together, our data are consistent with an overall sacrifice of the NAD^+ and NADH pools and mitochondrial oxidation–reduction activity in favor of NADPH generation and MQ elimination, a scenario that was highly exaggerated under glucose-limiting conditions (Fig. 7). The exaggerated responses at low-glucose states underscore a central role for glucose in cellular ATP and pyridine nucleotide homeostasis and mitochondrial functional integrity.

Quinone-induced NAD(H)-to-NADP(H) interconversion has been documented in hepatocytes (34) and in nonmammalian

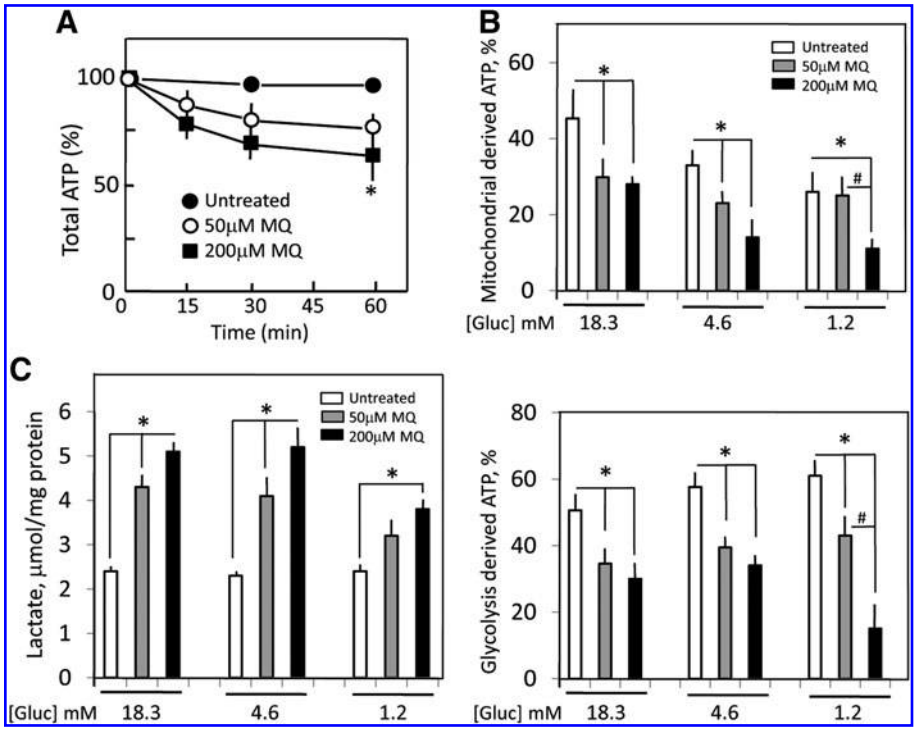

FIG. 5. MQ-induced changes in cellular ATP and cytosolic lactate. HT29 cells (1×10^4) were seeded in 96-well plates and grown overnight at 37°C. The next day, the culture media were replaced by fresh phenol-red and fetal bovine serum-free Dulbecco's modified essential medium containing 1.2, 4.6, or 18.3 m*M* glucose, and the cells were exposed to 50 or 200 μM MQ. **(A)** In time course experiments, cells were treated with MQ for 0–60 min. ATP was measured with a luciferin/luciferase bioluminescence Promega kit according to manufacturer's protocol. Each experiment was conducted in quadruplicates and ATP contents are expressed as percent relative to untreated controls (100%). Results are mean ± SEM for six cell preparations. **(B)** The contribution of mitochondria-derived (*upper panel*) and glycolysis-derived (*bottom panel*) ATP to total ATP levels was determined in cells treated with antimycin A (2 μM) or 2-deoxyglucose (2DG), respectively. Concentrations of 2DG, namely, 3, 11.5, and 45.8 m*M* were 2.5×higher than the respective glucose concentrations. Results are mean ± SEM for $n=6$ for 18.3 m*M* glucose, and $n=4$ each for 4.6 and 1.2 m*M* glucose. $^*p<0.05$ versus untreated control; $^{\#}p<0.05$ versus 50 μM MQ. **(C)** Cytosolic lactate in cells treated with 50 and 200 μM MQ at various glucose concentrations. Results are expressed as μmol/mg protein and are mean ± SEM for three cell preparations. $^*p<0.05$ versus untreated control.

cells (31). Our results show that in HT29 cells, NADPH decreases concurrent with $NADP^+$ increases, and NAD^+ loss within the cytosol is consistent with increased NAD^+-to-$NADP^+$ conversion and enhanced NADPH consumption. Parallel NADH decreases in the face of NADPH loss and $NADP^+$ increase within the mitochondria is consistent with NADH-to-NADPH conversion and increased NADPH utilization. The finding that decreases in cytosolic and mitochondrial NADPH occurred despite increases in $NADP^+$ and stimulation of NADPH-generating enzymes suggests that the consumption of NADPH far exceeded that of NADPH availability for MQ metabolism. Cellular NADPH supply rate is likely to reach critically low levels even at mild MQ stress under reduced glucose conditions. We previously demonstrated that the supply of NADPH was rate-limiting for the reduction of *tert*-butylhydroperoxide in isolated enterocytes (3). Interestingly, in isolated hepatocytes, steady-state NADPH levels increased after treatment with similar MQ doses (100–200 μM), indicating that liver cells exhibited a high capacity for NADPH generation during oxidative challenge (32, 33), consistent with a large hepatocellular glucose reserve. Thus, at a given oxidant load, the liver may be better able to withstand against oxidative tissue damage than the colon.

The disruption of pyridine nucleotide homeostasis and altered glucose status were associated with impairment of cytosolic and mitochondrial bioenergetics. Cellular ATP losses were attributed to decreases in both glycolysis-derived and mitochondrial ATP. MQ-induced decrease in ATP has previously been reported (34, 35) in conjunction with glutathione depletion (9, 28), protein oxidation (9, 23), and Ca^{2+} perturbations (12). The finding that aerobic glycolysis was stimulated by MQ (Fig. 5C) suggests that the Warburg effect will be prominent in cellular ATP homeostasis during oxidative challenge and compromised mitochondrial function in colon cancer cells. Our result that the magnitude of MQ-induced lactate formation was attenuated at low glucose suggests that decreased aerobic glycolysis under conditions of MQ stress and reduced glucose was the result of limited substrate flux through the pathway rather than an intrinsic effect of MQ on glycolysis.

Interestingly, a stable mitochondrial NAD^+ pool was maintained in normal glucose despite significant losses in mitochondrial NADH and ATP levels. The preservation of mitochondrial NAD^+ was reportedly critical to liver cell survival (28, 35). The significant loss of the NAD^+ pool in low glucose is notable. Our results are consistent with the view that different NADPH-generating pathways were responsible for the supply of reducing equivalents for MQ metabolism in normal and low-glucose states. Low-glucose flux decreased NADPH generation from the PPP under limiting glucose conditions. Hence, NADPH supply was derived from low yielding sources such as NAD^+/NADH pools and dehydrogenases that were inadequate for full reduction of MQ to HQ. Incomplete MQ reduction generated $SQ^{\bullet}$, which redox cycles readily to regenerate MQ, a process that consumed O_2 excessively (Fig. 1), independent of mitochondrial respiration. The findings of stimulated NNT and NADK activities (Table 1), elevated MQ-induced O_2 consumption (Fig. 6B), and increased P_{50} of O_2 dependence (Fig. 6A) are consistent with this scenario. In contrast, full MQ-to-HQ metabolism was met by a nonlimiting NADPH supply from the PPP, quantitatively the major

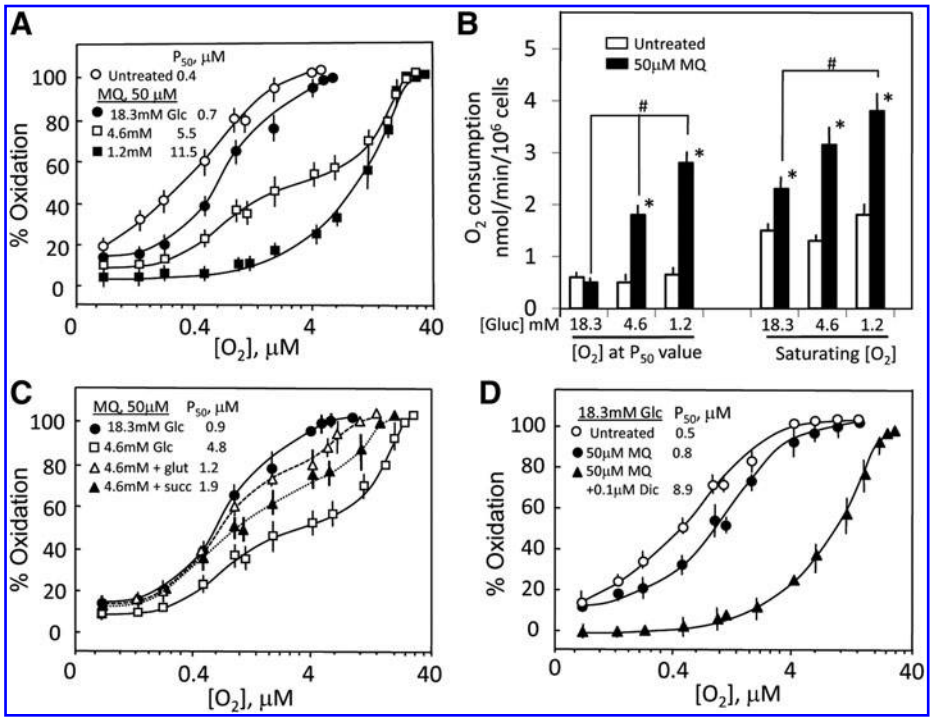

FIG. 6. MQ increases the P_{50} value of O_2 dependence of oxidation of mitochondrial pyridine nucleotides and O_2 consumption in HT29 cells. O_2 dependence of oxidation of NADH/NAD^+ was determined in HT29 cells (5×10^6/ml) in Gey's buffer containing 0, 1.2, 4.6, and 18.3 m*M* glucose in the absence or presence of 50 μM MQ. Whenever present, glutamate and succinate, and dicumarol were added to final concentrations of 10 m*M* and 0.1 μM, respectively. Cells were maintained in suspension by gentle stirring, and changes in oxidation–reduction of mitochondrial NADH/NAD^+ were measured by dual-wavelength spectrophotometry using wavelength pairs of 340–375 nm at various O_2 concentrations (4). Results are expressed as percent oxidation calculated with respect to aerobic cells; the P_{50} value represents half-maximal oxidation. Data are the mean ± SEM of the number of cell preparations for the following conditions: **(A)** 18.3 m*M* glucose, $n=4$; 4.6 m*M* glucose, $n=6$; 1.2 m*M* glucose, $n=4$. The O_2 dependences for non-MQ-treated controls at 4.6 and 1.2 m*M* glucose were similar to that of untreated control at 18.3 m*M* glucose (*open circle*) (data not shown for simplicity). **(C)** 18.3 m*M* glucose, $n=4$; 4.6 m*M* glucose, $n=6$; 1.2 m*M* glucose plus glutamate or succinate, $n=3$ each. The addition of glutamate and succinate in the absence of MQ gave O_2 dependences that were similar to those of 18.3 and 4.6 m*M* glucose without MQ (data not shown for simplicity). **(D)** 18.3 m*M* glucose ± dicumarol, $n=6$. O_2 dependence in presence of dicumarol alone without MQ was not different from 18.3 m*M* glucose without MQ. **(B)** MQ-induced increased in O_2 consumption rates were calculated from the oxidation–reduction tracings of mitochondrial pyridine nucleotides in cells exposed to 50 μM MQ in buffer containing various glucose concentrations. O_2 consumption rates were obtained at conditions of saturating [O_2] and at [O_2] at half-maximal oxidation (P_{50} values). Results are expressed as nmol/min/10^6 cells and are mean ± SEM for six cell preparations. $^*p<0.05$ versus untreated control; $^\#p<0.05$ versus 50 μM MQ in normal (18.3 m*M*) glucose.

cellular NADPH producer under conditions of glucose abundance (3, 18, 32), and an efficient cytosolic DT-diaphorase system (5, 42) (Fig. 1). This scenario is supported by findings of low MQ-induced O_2 consumption (Fig. 6B) and P_{50} of O_2 dependence (Fig. 6A), and a P_{50} value that was similar in magnitude to the low-glucose state when DT-diaphorase was inhibited (Fig. 6D). Based on this interpretation, significant losses in NAD^+ would be expected during glucose deficit (Fig. 3B), but not during glucose abundance except at high MQ dose (Fig. 2B). The finding that NAD^+ loss was greater than accounted for by increases in $NADP^+$ suggests that oxidative activation of other metabolic processes, such as polyADP ribosyl polymerase and sirtuin functions (1, 43, 44), could contribute to additional NAD^+ consumption. Direct effects of MQ on sirtuin (Sirt) protein activation or expression are unknown. Given that MQ induced significant NAD^+ loss, compromised Sirt-1 and Sirt-3 activities would cause the accumulation of acetylated proteins in the cytosol (and nucleus) and the mitochondria, respectively.

The unique O_2 dependence profile elicited in the presence of intermediate glucose (4.6 m*M*) reflected the combined influences of limited [O_2] for MQ-$SQ^\bullet$ redox cycling at low O_2 tension and limited [glucose] at high O_2 tension for NADPH-dependent MQ-to-HQ reduction. The transition phase that occurred between O_2 tension of 1 and 10 μM represented a state wherein there existed sufficient [O_2] to support MQ-$SQ^\bullet$ cycling but insufficient [glucose] to mediate NADPH-dependent MQ-to-HQ detoxication. In this regard, supplementation with succinate or glutamate induced left shifts in the O_2 dependence that resembled the profile under normal glucose. This means that exogenous supply of mitochondrial substrates can bring about a glucose-sparing effect, and through increasing glucose availability for NADPH generation and MQ detoxication, restore mitochondrial O_2 dependence in glucose-deficient cells. The finding that the P_{50} O_2 dependence increased >10-fold in low glucose underscores the deleterious metabolic impact that heightened nonmitochondrial O_2 utilization, such as redox cycling, can have on mitochondrial respiratory activity within a cell. Thus, mitochondrial O_2 dependence can be viewed as a biologically relevant metabolic sensor of the presence of nonmitochondrial O_2-consuming reactions.

Since the activities of cellular enzymes critical to NADPH generation were assayed under optimal conditions, it remains to be determined if the increases in G6PDH, NNT, and NADK activities reflected intracellular activities. It is also unresolved whether enzyme activation was the result of NADPH

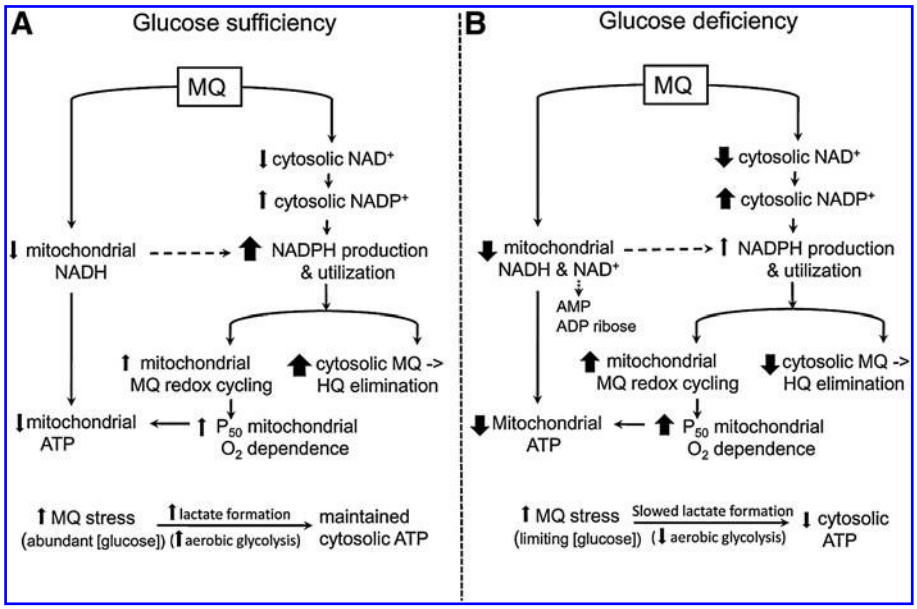

FIG. 7. MQ and low glucose disrupt cytosolic and mitochondrial pyridine nucleotides and compromise cellular ATP and NADPH-dependent MQ metabolism. (A) In normal glucose, MQ-induced cytosolic NAD^+ loss occurs concurrently with increased $NADP^+$ pools and enhanced NADPH utilization in support of MQ elimination and redox cycling. Decreased mitochondrial NADH alongside cytosolic NAD^+-to-$NADP^+$ shift contributes to attenuated mitochondrial ATP production. Mitochondrial respiratory activity is further compromised by increased nonmitochondrial O_2 consumption by MQ redox cycling. MQ stress stimulates aerobic glycolysis (evidenced by increased cytosolic lactate concentrations) and maintains cytosolic ATP. **(B)** MQ-induced disruption in NADH/NAD^+ and NADPH/$NADP^+$ redox status is heightened under low-glucose conditions. In addition, glucose lack limits NADPH generation and cytosolic MQ elimination. This scenario increases mitochondrial MQ redox cycling potential, which decreases O_2 availability for oxidation–reduction activity. A compromised mitochondrial O_2 dependence coupled to an exaggerated loss of mitochondrial NADH dramatically decreased mitochondrial ATP. During MQ stress, slowed aerobic glycolysis under limiting glucose conditions results in decreased cytosolic ATP.

depletion, increased oxidative stress, post-translational modifications, or increased protein amounts. Regardless of mechanism, the stimulation of NADK was central to NAD^+-to-$NADP^+$ conversion and cellular NADPH maintenance. The regulation of cytosolic human NADK (hNADK) is poorly understood despite extensive studies in prokaryotes, yeasts, and plants (25, 26). The kinetic parameters of hNADK, K_M of 0.5 m*M* for NAD^+ and 3 m*M* for ATP, are close to physiological concentrations of these substrates (20), suggesting that substrate variations would alter enzyme activity. NADPH may be an inhibitor of hNADK in HEK293 cells (26). However, in contrast to our current findings, neither kinase activity nor expression was stimulated by H_2O_2 or MQ in these cells, which suggests that control of NADK may be cell type specific. It is noteworthy that HEK293 cells exhibited low basal NADK activity, yet resistant to oxidative stress (26).

In summary, our current study provides the first evidence linking an oxidative stress-induced acute metabolic impairment to a disrupted pyridine nucleotide redox system in colon cancer cells. The biological significance of these findings for other cell types with high NADPH requirement has not been fully explored. For instance, activation of NADPH oxidase in neutrophils during oxidative burst imposes a high demand for cellular NADPH. What this loss of NADPH homeostasis means for cellular bioenergetics is unclear since neutrophils exhibit few mitochondria that are restricted to a role in apoptosis rather than to ATP production (22, 38). The delineation of the relationships among oxidative stress, NADPH utilization, and implications for cellular bioenergetics should provide interesting insights into the link between redox biology and energy metabolism not only in colonic and inflammatory cells, but also in a variety of other cell types with high metabolic demands.

Acknowledgment

This work was supported by a grant from the National Institutes of Health, DK44510.

Author Disclosure Statement

The authors declare no conflict of interest.

References

1. Alano CC, Ying W, and Swanson RA. Poly(ADP-ribose) polymerase-1-mediated cell death in astrocytes requires NAD+ depletion and mitochondrial permeability transition. *J Biol Chem* 279: 18895–18902, 2004.
2. Andersson BS and Jones DP. Use of digitonin fractionation to determine mitochondrial transmembrane ion distribution in cells during anoxia. *Anal Biochem* 146: 164–172, 1985.
3. Aw TY and Rhoads CA. Glucose regulation of hydroperoxide metabolism in rat intestinal cells. Stimulation of reduced nicotinamide adenine dinucleotide phosphate supply. *J Clin Invest* 94: 2426–2434, 1994.
4. Aw TY, Wilson E, Hagen TM, and Jones DP. Determinants of mitochondrial O2 dependence in kidney. *Am J Physiol* 253: F440–F447, 1987.
5. Cadenas E. Antioxidant and prooxidant functions of DT-diaphorase in quinone metabolism. *Biochem Pharmacol* 49: 127–140, 1995.
6. Circu ML and Aw TY. Glutathione and apoptosis. *Free Radic Res* 42: 689–706, 2008.
7. Circu ML and Aw TY. Reactive oxygen species, cellular redox systems, and apoptosis. *Free Radic Biol Med* 48: 749–762, 2010.
8. Circu ML, Moyer MP, Harrison L, and Aw TY. Contribution of glutathione status to oxidant-induced mitochondrial

DNA damage in colonic epithelial cells. *Free Radic Biol Med* 47: 1190–1198, 2009.
9. Circu ML, Rodriguez C, Maloney R, Moyer MP, and Aw TY. Contribution of mitochondrial GSH transport to matrix GSH status and colonic epithelial cell apoptosis. *Free Radic Biol Med* 44: 768–778, 2008.
10. Flint AP and Denton RM. The role of nicotinamide-adenine dinucleotide phosphate-dependent malate dehydrogenase and isocitrate dehydrogenase in the supply of reduced nicotinamide-adenine dinucleotide phosphate for steroidogenesis in the superovulated rat ovary. *Biochem J* 117: 73–83, 1970.
11. Freeman H, Shimomura K, Cox RD, and Ashcroft FM. Nicotinamide nucleotide transhydrogenase: a link between insulin secretion, glucose metabolism and oxidative stress. *Biochem Soc Trans* 34: 806–810, 2006.
12. Frei B, Winterhalter KH, and Richter C. Menadione- (2-methyl-1,4-naphthoquinone-) dependent enzymatic redox cycling and calcium release by mitochondria. *Biochemistry* 25: 4438–4443, 1986.
13. Jain M, Brenner DA, Cui L, Lim CC, Wang B, Pimentel DR, Koh S, Sawyer DB, Leopold JA, Handy DE, Loscalzo J, Apstein CS, and Liao R. Glucose-6-phosphate dehydrogenase modulates cytosolic redox status and contractile phenotype in adult cardiomyocytes. *Circ Res* 93: e9–e16, 2003.
14. Jo SH, Son MK, Koh HJ, Lee SM, Song IH, Kim YO, Lee YS, Jeong KS, Kim WB, Park JW, Song BJ, and Huh TL. Control of mitochondrial redox balance and cellular defense against oxidative damage by mitochondrial NADP+-dependent isocitrate dehydrogenase. *J Biol Chem* 276: 16168–16176, 2001.
15. Johnson D and Lardy H. Isolation of Liver or Kidney Mitochondria. *Method Enzymol* 10: 94–96, 1967.
16. Jones DP. Disruption of mitochondrial redox circuitry in oxidative stress. *Chem Biol Interact* 163: 38–53, 2006.
17. Klaidman LK, Leung AC, and Adams JD Jr. High-performance liquid chromatography analysis of oxidized and reduced pyridine dinucleotides in specific brain regions. *Anal Biochem* 228: 312–317, 1995.
18. Krebs HA and Eggleston LV. The regulation of the pentose phosphate cycle in rat liver. *Adv Enzyme Regul* 12: 421–434, 1974.
19. Lee SM, Koh HJ, Park DC, Song BJ, Huh TL, and Park JW. Cytosolic NADP(+)-dependent isocitrate dehydrogenase status modulates oxidative damage to cells. *Free Radic Biol Med* 32: 1185–1196, 2002.
20. Lerner F, Niere M, Ludwig A, and Ziegler M. Structural and functional characterization of human NAD kinase. *Biochem Biophys Res Commun* 288: 69–74, 2001.
21. Lowry OH and Passonneau J. *A Flexible System of Enzymatic Analysis*. NY: Academic Press, 194–211, 1972.
22. Maianski NA, Geissler J, Srinivasula SM, Alnemri ES, Roos D, and Kuijpers TW. Functional characterization of mitochondria in neutrophils: a role restricted to apoptosis. *Cell Death Differ* 11: 143–153, 2004.
23. Mirabelli F, Salis A, Perotti M, Taddei F, Bellomo G, and Orrenius S. Alterations of surface morphology caused by the metabolism of menadione in mammalian cells are associated with the oxidation of critical sulfhydryl groups in cytoskeletal proteins. *Biochem Pharmacol* 37: 3423–3427, 1988.
24. Nisselbaum JS, and Green S. A simple ultramicro method for determination of pyridine nucleotides in tissues. *Anal Biochem* 27: 212–217, 1969.
25. Pollak N, Dolle C, and Ziegler M. The power to reduce: pyridine nucleotides—small molecules with a multitude of functions. *Biochem J* 402: 205–218, 2007.
26. Pollak N, Niere M, and Ziegler M. NAD kinase levels control the NADPH concentration in human cells. *J Biol Chem* 282: 33562–33571, 2007.
27. Pongratz RL, Kibbey RG, Shulman GI, and Cline GW. Cytosolic and mitochondrial malic enzyme isoforms differentially control insulin secretion. *J Biol Chem* 282: 200–207, 2007.
28. Redegeld FA, Moison RM, Koster AS, and Noordhoek J. Alterations in energy status by menadione metabolism in hepatocytes isolated from fasted and fed rats. *Arch Biochem Biophys* 273: 215–222, 1989.
29. Reed DJ, Babson JR, Beatty PW, Brodie AE, Ellis WW, and Potter DW. High-performance liquid chromatography analysis of nanomole levels of glutathione, glutathione disulfide, and related thiols and disulfides. *Anal Biochem* 106: 55–62, 1980.
30. Shimomura K, Galvanovskis J, Goldsworthy M, Hugill A, Kaizak S, Lee A, Meadows N, Quwailid MM, Rydstrom J, Teboul L, Ashcroft F, and Cox RD. Insulin secretion from beta-cells is affected by deletion of nicotinamide nucleotide transhydrogenase. *Methods Enzymol* 457: 451–480, 2009.
31. Singh R, Lemire J, Mailloux RJ, and Appanna VD. A novel strategy involved in [corrected] anti-oxidative defense: the conversion of NADH into NADPH by a metabolic network. *PLoS One* 3: e2682, 2008.
32. Smith PF, Alberts DW, and Rush GF. Menadione-induced oxidative stress in hepatocytes isolated from fed and fasted rats: the role of NADPH-regenerating pathways. *Toxicol Appl Pharmacol* 89: 190–201, 1987.
33. Smith PF, Alberts DW, and Rush GF. Role of glutathione reductase during menadione-induced NADPH oxidation in isolated rat hepatocytes. *Biochem Pharmacol* 36: 3879–3884, 1987.
34. Stubberfield CR and Cohen GM. Interconversion of NAD(H) to NADP(H). A cellular response to quinone-induced oxidative stress in isolated hepatocytes. *Biochem Pharmacol* 38: 2631–2637, 1989.
35. Stubberfield CR and Cohen GM. NAD+ depletion and cytotoxicity in isolated hepatocytes. *Biochem Pharmacol* 37: 3967–3974, 1988.
36. Tribble DL and Jones DP. Oxygen dependence of oxidative stress. Rate of NADPH supply for maintaining the GSH pool during hypoxia. *Biochem Pharmacol* 39: 729–736, 1990.
37. Umemura K and Kimura H. Determination of oxidized and reduced nicotinamide adenine dinucleotide in cell monolayers using a single extraction procedure and a spectrophotometric assay. *Anal Biochem* 338: 131–135, 2005.
38. van Raam BJ, Verhoeven AJ, and Kuijpers TW. Mitochondria in neutrophil apoptosis. *Int J Hematol* 84: 199–204, 2006.
39. Vander Heiden MG, Cantley LC, and Thompson CB. Understanding the Warburg effect: the metabolic requirements of cell proliferation. *Science* 324: 1029–1033, 2009.
40. von Kleist S, Chany E, Burtin P, King M, and Fogh J. Immunohistology of the antigenic pattern of a continuous cell line from a human colon tumor. *J Natl Cancer Inst* 55: 555–560, 1975.
41. Wagner TC and Scott MD. Single extraction method for the spectrophotometric quantification of oxidized and reduced pyridine nucleotides in erythrocytes. *Anal Biochem* 222: 417–426, 1994.
42. Wefers H and Sies H. Hepatic low-level chemiluminescence during redox cycling of menadione and the menadione-glutathione conjugate: relation to glutathione and NAD(P)H:quinone reductase (DT-diaphorase) activity. *Arch Biochem Biophys* 224: 568–578, 1983.

43. Yang H, Yang T, Baur JA, Perez E, Matsui T, Carmona JJ, Lamming DW, Souza-Pinto NC, Bohr VA, Rosenzweig A, de Cabo R, Sauve AA, and Sinclair DA. Nutrient-sensitive mitochondrial NAD+ levels dictate cell survival. *Cell* 130: 1095–1107, 2007.
44. Ying W, Alano CC, Garnier P, and Swanson RA. NAD+ as a metabolic link between DNA damage and cell death. *J Neurosci Res* 79: 216–223, 2005.

Address correspondence to:
Dr. Tak Yee Aw
Department of Molecular and Cellular Physiology
LSU Health Sciences Center
1501 Kings Highway
Shreveport, LA 71130-3932

E-mail: taw@lsuhsc.edu

Date of first submission to ARS Central, July 15, 2010; date of final revised submission, November 09, 2010; date of acceptance, November 14, 2010.

Abbreviations Used

2DG = 2-deoxyglucose
DMEM = Dulbecco's modified essential medium
DT = DT-diaphorase
FBS = fetal bovine serum
G6PDH = glucose-6-phosphate dehydrogenase
GSH = glutathione
GSSG = glutathione disulfide
HPLC = high-performance liquid chromatography
HQ = hydroquinone
ICDH = isocitrate dehydrogenase
ME = malic enzyme
MQ = menadione
$NADH/NAD^+$ = reduced and oxidized nicotinamide adenine dinucleotide
NADK = NAD kinase
$NADPH/NADP^+$ = reduced and oxidized nicotinamide adenine dinucleotide phosphate
NNT = nicotinamide nucleotide transhydrogenase
PPP = pentose phosphate pathway
SEM = standard error of the mean
$SQ^\bullet$ = semiquinone radical

This article has been cited by:

1. Magdalena L. Circu, Tak Yee Aw. 2012. Intestinal redox biology and oxidative stress. *Seminars in Cell & Developmental Biology* **23**:7, 729-737. [CrossRef]
2. Hao Wu, Zonghui Ding, Danqing Hu, Feifei Sun, Chunyan Dai, Jiansheng Xie, Xun Hu. 2012. Central role of lactic acidosis in cancer cell resistance to glucose deprivation-induced cell death. *The Journal of Pathology* n/a-n/a. [CrossRef]
3. Magdalena L. Circu, Tak Yee Aw. 2011. Redox biology of the intestine. *Free Radical Research* 1-22. [CrossRef]